



EXPERIMENTAL AND SIMULATIVE ASSESSMENT OF CRASHWORTHINESS OF MECHANICALLY AGED SHORT- FIBRE REINFORCED THERMOPLASTICS

Witzgall, Christian; Wartzack, Sandro

Friedrich-Alexander-University Erlangen-Nuremberg, Germany

Abstract

Short-fibre reinforced thermoplastics (SFRT) are increasingly used in 21st century's automotive construction. Besides statically loaded parts, SFRT are also used for safety-relevant components such as door modules and crash absorbers. Temperature, chemically aggressive media as well as mechanical loading lead to aging effects within the plastic, which generally, weakens the material's mechanical properties. Thus, within the present paper, a series of tests is introduced in order to investigate the effect of mechanical ageing on the material's crashworthiness behaviour. Furthermore, a concept for consideration the effects of ageing within numerical simulation is introduced.

Keywords: Simulation, Design for X (DfX), Numerical methods, Crashworthiness, Safety

Contact:

Christian Witzgall

Friedrich-Alexander-University Erlangen-Nuremberg

Engineering Design

Germany

witzgall@mfk.fau.de

Please cite this paper as:

Surnames, Initials: *Title of paper*. In: Proceedings of the 21st International Conference on Engineering Design (ICED17), Vol. 1: Resource-Sensitive Design | Design Research Applications and Case Studies, Vancouver, Canada, 21.-25.08.2017.

1 INTRODUCTION

Short-fibre reinforced thermoplastics (SFRT) are increasingly used in 21st century's automotive engineering. SFRT are not only used for statically loaded parts, but also for safety-relevant components such as engine mounts, door modules and crash absorbers (LANXESS Germany, 2004; Short and Tullo, 2007). Kamber (2005) shows an examination of the crashworthiness of used vehicles. In the examination used vehicles were tested in a frontal impact load case under the same testing conditions as before their introduction to the market (55 km/h impact velocity, 50 percent overlap). The twelve year old model Toyota Corolla 1.6 Si had significantly increased values in comparison to the new vehicle regarding the loads acting on the driver. Figure 1 demonstrates the course of the resultant head acceleration, which is increased by about 20 percent in the used vehicle and thus exceeds the permitted Head Injury Criterion. The examination concludes that the increased loads can be explained by "the ageing process of the entire vehicle". (Kamber, 2005)

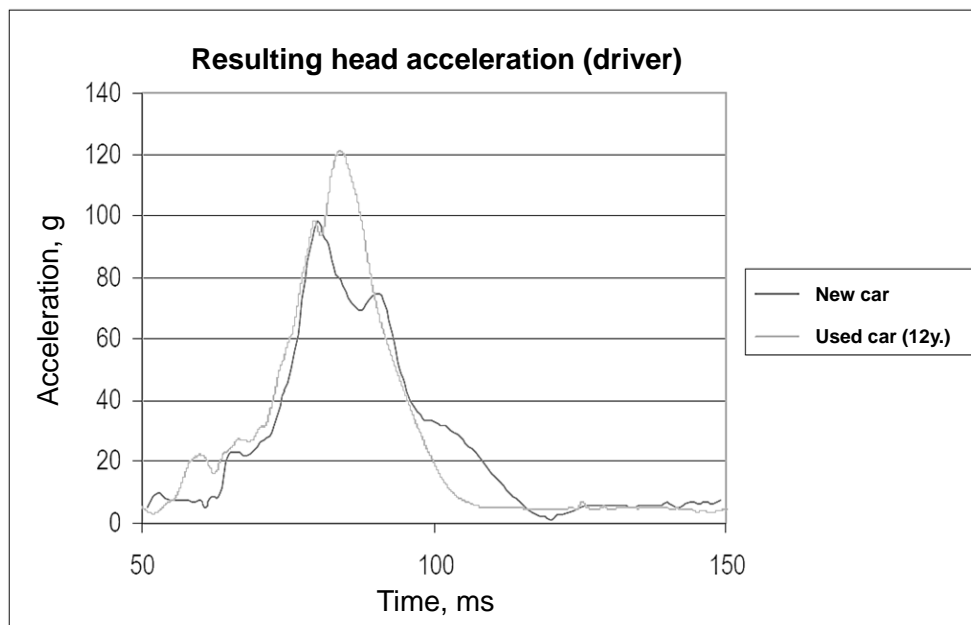


Figure 1. resulting head acceleration in used vehicle and new vehicle (Kamber, 2005)

Similar observations are described by (Blows *et al.*, 2003) and (Anderson *et al.*, 2009). According to these Australian studies, the risk of car crash injury increases with older vehicle year. Although it is undisputed that there are numerous effects influencing vehicle safety, ageing of plastic components within the vehicle is rarely addressed.

Regarding plastics, factors such as temperature, radiation exposure, media load as well as mechanical loads lead to an ageing process which generally deteriorates the mechanical material properties (Martin, 2008).

Thus, within the present paper, a study is presented which examines the ageing process of short-fibre reinforced thermoplastics as a result of mechanical loads. Furthermore the influence of the ageing process on the material behaviour under impact load is examined. It is to be demonstrated that the mechanical pre-existing damage has a considerable effect on the capacity of the material to withstand stresses under highly dynamic conditions. Finally, a concept for consideration the effects of ageing within numerical simulation of plastic parts, especially with fibre reinforcement, is introduced.

2 EXPERIMENTAL STUDY

The experiments presented within this chapter were carried out in order to examine the effects of ageing on the crashworthiness parameters of SFRT. (Witzgall and Wartzack, 2016)

2.1 Testing condition and test realisation

A polybutylene terephthalate blend (PBT) with 30 percent short-fibre reinforcement is used for the following experiments. All experiments were conducted at room temperature. All specimens used are of the same age and were processed and stored under the same conditions. Thus the ageing effects caused by temperature, radiation or media load shall be minimised as much as possible.

Figure 2 schematically shows the steps of this series of experiments. Firstly the strength, the rigidity and the elongation at break were determined for new specimens in quasi-static tensile tests. The results from these tests were used to determine the loading conditions for the determination of the maximal number of cycles endured. At 1/3 or 2/3 respectively of the quasi-statically measured maximum stress, several specimen were put under a pulsating tensile stress until they break. The same load levels are also employed regarding the prior damages, however, the chosen number of circles endured is significantly smaller than the number of cycles which was at least endured in prior experiments. The two different load levels with a prior damage in different stages and the intact specimens result in three series, 0, 1, and 2. They are compared in high velocity tensile tests at 2.0 m/s.

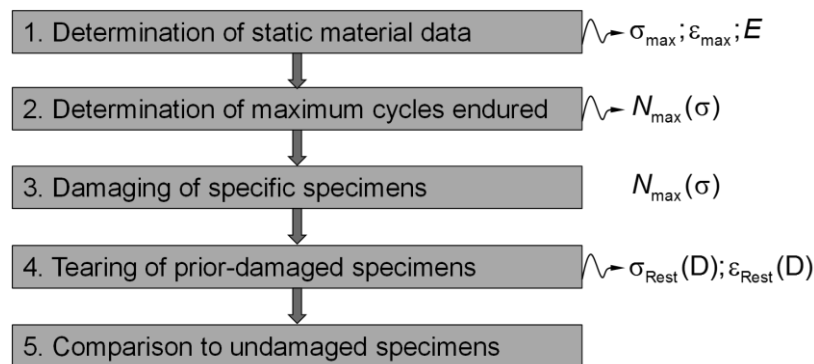


Figure 2. stepwise testing procedure

All experiments are conducted with specimens according to Becker (2009) as displayed in Figure 3. Those specimens have a thickness of 3.5 mm and their geometrical shape is particularly suitable for high velocity tensile tests. The very short initial length makes it possible to reach high strain rates already at moderate velocities and to create an ideally uniaxial state of stress in the central part of the specimen. In addition, the relatively broad surface of the specimen is ideal for a reliable and repeatable strain analysis. (Becker, 2009)

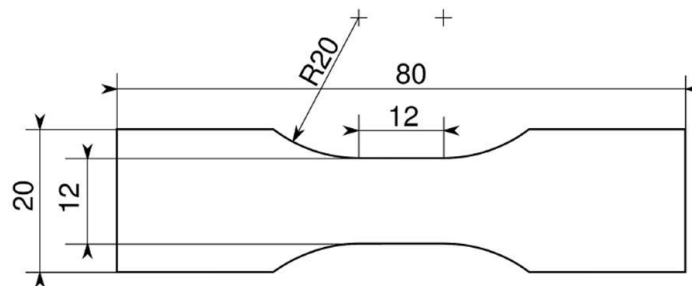


Figure 3. Test specimen according to Becker, 2009

The same shape of specimen is also used for the quasi-statically and cyclically conducted experiments to avoid an influence of the shape on the results.

All steps of the experiment are described in the following. A further chapter presents the results of the highly dynamic tensile tests and the comparison of intact specimen to those with prior damage.

2.2 Determination of static material parameters

To characterise the material under static loads uniaxial tension tests are carried out at a testing velocity of 0.001 m/s. In relation to the length of the central part of the specimen this gives a nominal strain rate of 0.08 s^{-1} , which can be categorised as quasi-static. To provide a better statistical basis the experiments are repeated ten times; the results are averaged and listed in Table 1 with standard deviation.

Table 1. Static material parameters

Tensile Rigidity $E_{0,2\%}$	Maximum Stress σ_{\max}	Elongation at Break ε_{\max}
10,300 ± 480 MPa	113 ± 3.4 MPa	1.8 ± 0.08 %

With the in average maximally endured tensile stresses two stress levels are defined as in Equation(1):

$$\kappa_{\sigma} = \frac{\sigma_0}{\sigma_{\max}}; \quad \kappa_1 = 0.66; \quad \kappa_2 = 0.33 \quad (1)$$

They determine the load applied in the fatigue test.

2.3 Determination of the number of cycles endured

The maximal number of cycles endured is to be calculated in cyclic fatigue tests at the respective load levels κ_1 and κ_2 . These tests are performed on a servo-hydraulic pulsator with a loading frequency of 5 Hz. Due to hysteresis effects of the thermoplastics a higher testing frequency is not attainable, as the heat generated by internal friction would cause an intolerable elevation of temperature and thus a softening of the material. All experiments are carried force-controlled and with pulsating tensile stresses. The ratio of upper and lower tensile stress therefore is (Equation(2)):

$$R = \frac{\sigma_u}{\sigma_o} \approx 0 \quad (2)$$

Figure 4 shows the number of cycles endured until the specimen breaks. For the load level $\kappa_1 = 0.66$ the numbers are between $2.1 \dots 3.4 \cdot 10^5$ and for $\kappa_2 = 0.33$ they are between $5.5 \dots 7.2 \cdot 10^5$.

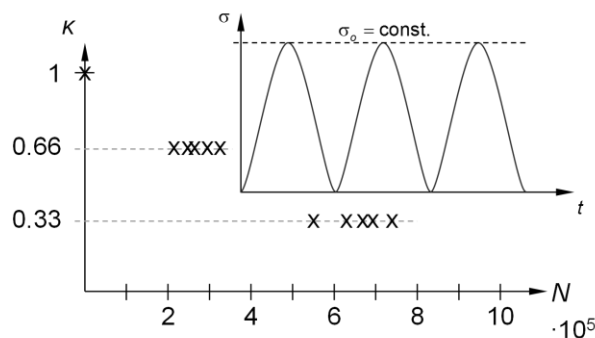


Figure 4. number of cycles endured until break, depending on load level

Because of the small number of experiments with only 5 specimens there is no calculation of chances of survival or any other statistical evaluation at this point. Instead the minimum number of cycles endured is used as a reference value for the following experiments:

$$\begin{aligned} N_1(\kappa_1 = 0.66) &= 2.1 \cdot 10^5 \\ N_2(\kappa_2 = 0.33) &= 5.5 \cdot 10^5 \end{aligned} \quad (3)$$

2.4 Mechanical ageing of single specimen

To achieve mechanical ageing of the specimens a servo-hydraulic pulser is used, such as in the cyclic fatigue tests. In this case it is crucial that the specimens do not already break in the cyclic test. Additionally it should be avoided that regardless of the different load levels the ageing is equally pronounced in both series of specimen.

Therefore, the principle of damage accumulation is introduced for quantification of the ageing within the specimens. Hence, hereafter the term damage will be used. Within the test series, the linear damage accumulation developed by Palmgren and Miner (Palmgren, 1924; Miner, 1945, 1959) will be used. It quantifies the damage parameter D by summing up the ratio of cycles endured to maximum number of endurable cycles for a certain load spectrum as shown in Equation (4).

$$D = \sum_i \frac{n_i}{N_i} \quad (4)$$

So-called sequence effects, i.e. the order in which the different load spectra occurred, as well as non-linear behaviour cannot be taken into account by the linear damage accumulation (Jollivet *et al.*, 2013). However, for every test series, only one stress level is used, thus qualifying the method for this first examination.

The definition of the series of specimen and their degrees of damage are listed in Table 2. Series 1 was loaded at a higher load level, but with a smaller number of cycles, whereby series 2 was loaded at a lower load level, but with a higher number of cycles. This resulted in a lower degree of damage for series 1. Series 0 represents the intact control group.

Table 2. Experimental parameters of the series of specimen

series	load level	number of cycles	max. number of cycles endured	degree of damage
0	no prior damage			
1	$\kappa_1 = 0.66$	$n_1 = 81,000$	$N_1 = 213,000$	$D_1 \approx 0.4$
2	$\kappa_2 = 0.33$	$n_2 = 324,000$	$N_2 = 550,000$	$D_2 \approx 0.6$

2.5 Comparison of previously damaged and un-damaged specimens in high-velocity tensile tests

A servo-hydraulic high velocity testing facility is used to achieve the final tearing of the three series of specimens. Therefore uniaxial tensile test are performed with a testing velocity of 2.0 m/s, five specimens of each of the series 1 and 2 as well as ten specimens of the series 0 are tested. All tests are conducted at room temperature with a random order.

Table 3 shows the stresses and strains endured by each of the series of specimens in the tensile tests. The maximum stress endured by the specimens decreases with an increasing degree of damage: the intact series 0 endures an averaged maximum stress of 119 MPa, whereas this value is with 91 MPa 23 percent lower in series 1 and with 84 MPa 30 percent lower in series 2. A similar development exists regarding the elongation at break, it also decreases with the progressing mechanical ageing process. Consequently also the energy absorbed by the specimens decreases. This was calculated by numerical integration of the recorded force-displacement-curves.

Table 3. Stresses and strains endured of the series of specimen

	series 0	series 1 ($D=0.4$)	series 2 ($D=0.6$)
σ_{Rest}	119 ± 3.2 MPa	91 ± 5.4 MPa (-23 %)	84 ± 4.1 MPa (-30 %)
$\varepsilon_{\text{Rest}}$	1.61 %	1.25 % (-22 %)	0.76 % (-43 %)
E_{abs}	855 Nmm	469 Nmm (-55 %)	174 Nmm (-79 %)

Figure 5 displays the stress-strain-curves as they were measured for the three series of specimen. The capacity of the material to absorb energy can also be estimated with this figure. The energy afforded to tear the specimens corresponds to the space under a force-displacement-curve. Thus the stress-strain-diagram also displays the reduction of energy absorption.

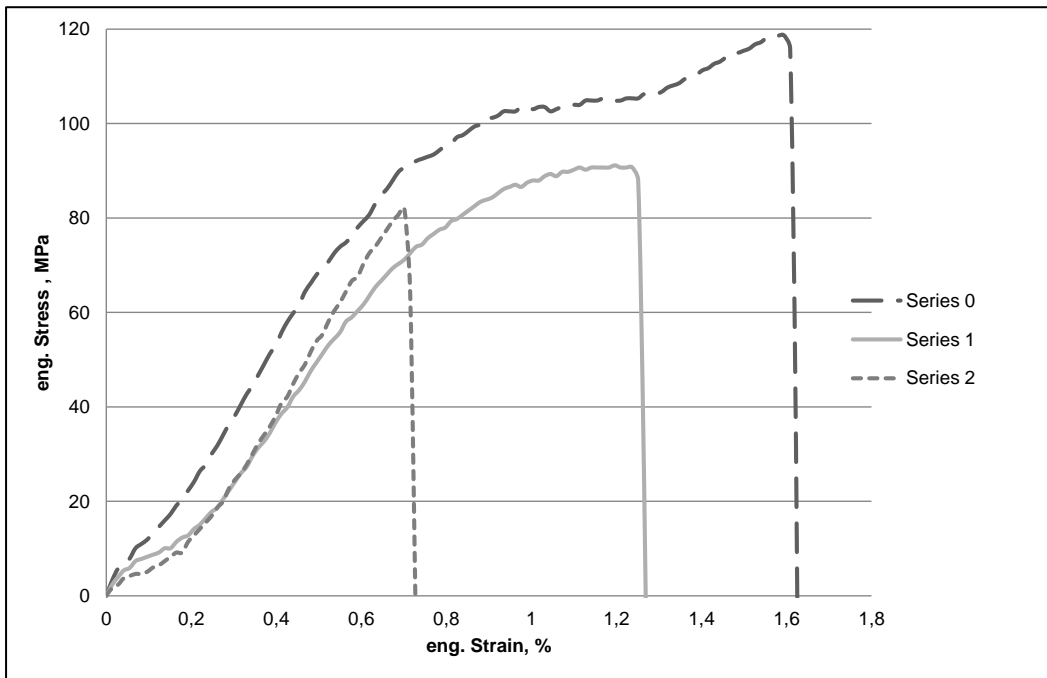


Figure 5. Stress-strain-diagrams (averaged) of the series 0, 1, and 2

Figure 6 shows microscopic images of the fractured surfaces of the specimens in 10-fold and 25-fold magnification. The left part of the picture shows the fractured surface of a torn specimen, which had no prior damage (series 0). The rugged surface is already visible to the naked eye. The right part of the picture shows the fractured surface of a specimen with prior damage from series 2. Also in this case the rugged surface of the specimen is visible to the naked eye. Additionally the examination with the optical microscope reveals short fibres which are torn out of the matrix. The images of the fractures are replicable regarding the different specimens of the three series. Conclusions can be drawn from the observation of these images of the torn specimens regarding material failure. According to the studies of Lawrence (1972) and Kim *et al.* (1992) a so-called fibre-pullout can be observed at this point, which is typical for short fibre reinforced thermoplastics, after the connection between the fibre material and the matrix material has been cut.

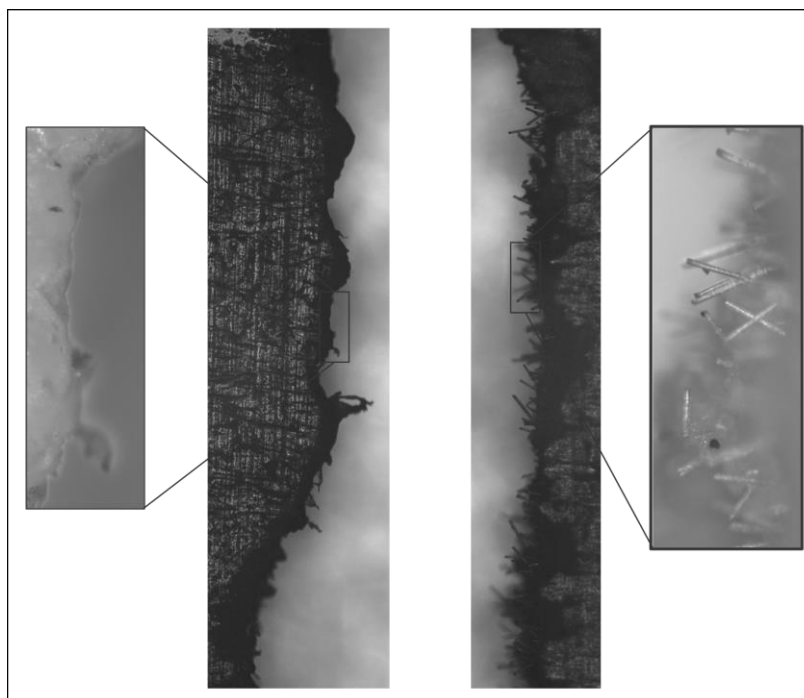


Figure 6. Microscopic images of the specimens with (right) and without (left) prior damage

3 CONSIDERING THE EFFECTS OF MECHANICAL AGEING WITHIN NUMERICAL SIMULATION

The findings of the experiments described above suggest a need for action towards considering the effects of mechanical ageing within numerical simulation, especially within the simulation of crash scenarios, thus allowing an assessment of vehicle crashworthiness within the whole span of life of a vehicle. Hence, a concept to meet this demand will be presented within the following.

Figure 7 gives an overview of the steps required to estimate the crashworthiness of structural components made of SFRT within the whole of their lifetime.

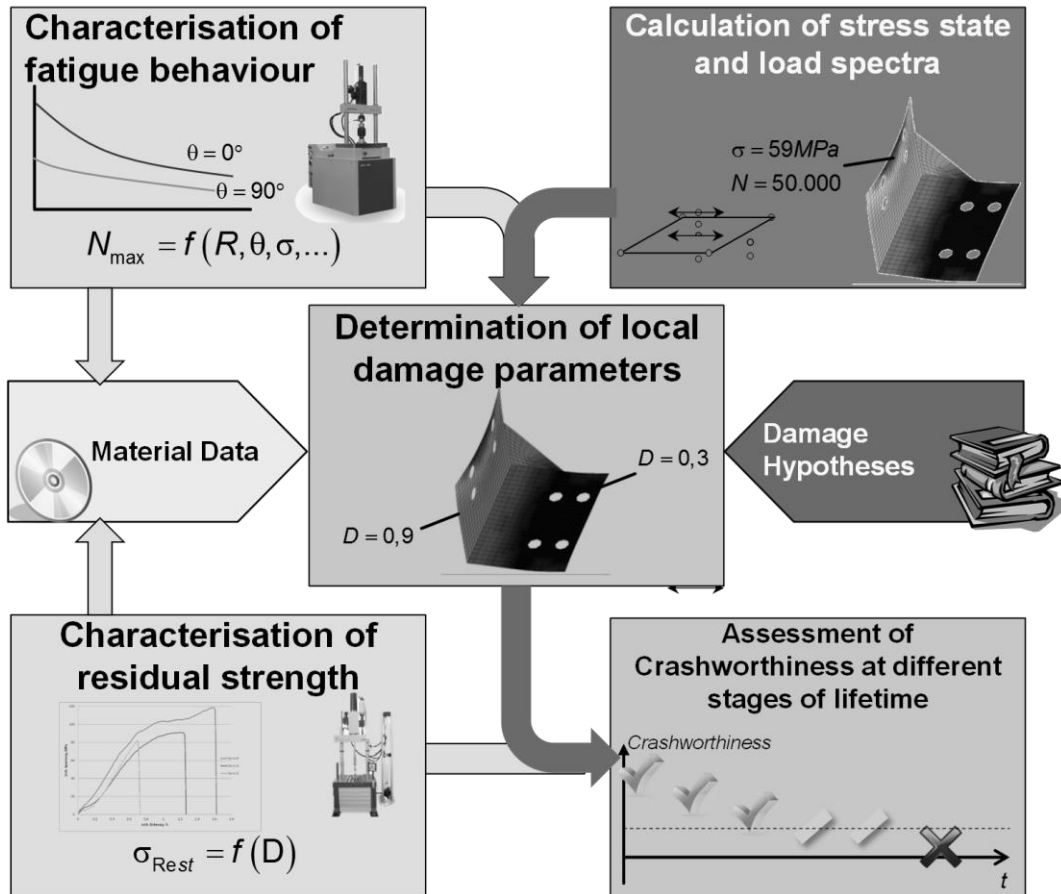


Figure 7. Steps required towards consideration of mechanical ageing in simulative crashworthiness evaluation

For quantification of the level of damage, different hypotheses from literature are to be evaluated. As stated before, the linear damage accumulation according to Palmgren and Miner was able to satisfy the needs for a first series of testing, namely comparing the damage induced for two different settings. However, it does not prove to be sufficient to describe SFRT's behaviour correctly enough, as it does not take the material's nonlinear behaviour into account.

Consequently, experimental characterisation of the material's fatigue behaviour is required. This especially includes the determination of the maximum number of cycles endured, depending on parameters such as stress ratio R and stress level σ , as well as the fibre orientation in order to take the anisotropic material behaviour into account. These experiments are to be carried out on a servohydraulic fatigue testing machine.

Further experiments are required to estimate the residual strength of specimen under highly dynamic load cases. Thus, the experimental scheme presented in chapter 2 will be repeated numerous, yielding information about residual strength and residual elongation at break in dependence of a certain level of damage.

The material data obtained from the cyclic and highly dynamic experiments are stored within a database. They will be used for the later simulation and documentation.

The simulation process itself consists of three parts: firstly, a simulation of the components' regular usage is required in order to determine the actual stress state within the part. According to (Gruber *et al.*, 2011), a static structural analysis is performed taking into account the fibre distribution within the part (Advani and Tucker, 1987). Different load cases and different numbers of loading cycles have to be considered as load spectra. As a second step, the local damage within the part, caused by normal usage, is calculated using the local stress states from the static structural analysis and damage hypotheses, e.g. from literature. Using the material's residual strength in accordance to damage, as shown in Figure 5 before, a crash simulation can be performed to evaluate a vehicle's crashworthiness at different stages of its lifetime.

3.1 Determination of local damage parameters – an example

The determination of local damage parameters will be explained using a simple example using a single finite element. The procedure is to be carried out for all finite elements within the model.

Let the finite element be statically loaded with a pulsating tensile stress σ_1 in fibre orientation direction. This stress state occurs in a number of n load cycles. From the experimental characterisation of fatigue behaviour, the maximum number of cycles endured for this stress level, $N_{\max}(\sigma_1)$, is known.

Hence, the fatigue damage $D(n, N_{\max}(\sigma_1))$ can be calculated using an appropriate damage hypothesis (Wu and Yao, 2010). The fatigue damage model used also takes the non-linear damage evolution into account, as seen in Figure 8.

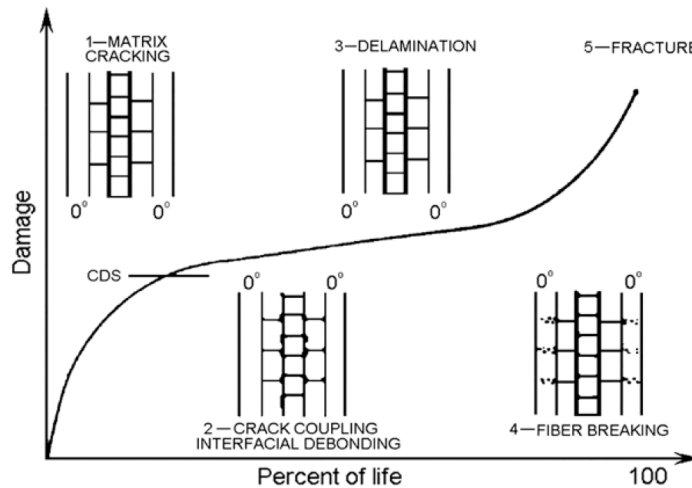


Figure 8. Fatigue damage evolution in composite laminates (Wu and Yao, 2010)

The degradation rule for the fatigue damage, $D(n)$ can be written as shown in Equation (5):

$$D(n) = \frac{E_0 - E(n)}{E_0 - E_f} = 1 - \left(1 - \left(\frac{n}{N} \right)^B \right)^A \quad (5)$$

where E_0 is initial Young's modulus, E_f is failure Young's modulus and $E(n)$ is Young's modulus of the material subjected to the n th cycle; A and B are model parameters which are to be determined experimentally (Wu and Yao, 2010).

Consequently, the damage within the finite element can be calculated.

From the experimental characterisation under high-velocity loading the residual strength is known in dependency of damage.

Thus, the material behaviour can be assigned correctly for the following crash simulation within every finite element.

4 CONCLUSION AND FUTURE RESEARCH

Within the present paper, an experimental study regarding the mechanical properties of pre-damaged specimens of short-fibre reinforced thermoplastics under high-velocity loading was introduced. To take

the effects of mechanical ageing into account, the specimens were loaded cyclically before being torn under elevated strain rates. Equivalent tests were carried out for intact specimen. As a result of this examination, the maximum endurable stress, strain and energy absorption decreased drastically for pre-damaged specimens.

To use the insights from experiments within crash simulation, a concept for the assessment of crashworthiness at different stages of lifetime was outlined. It uses the stress distribution within the part, calculated by finite element analysis, along with the number of occurring cycles to estimate the local damage within the part. Within this paper, damage hypotheses from literature dealing with carbon fibre reinforced plastics were used.

The results of the high-velocity tests are used to assign the material's behaviour correctly for each finite element within the part. Thus, a possible weakening of the part's crashworthiness due to mechanical ageing can be taken into account.

An important task for future research will be to further investigate the influence of ageing in dependency of fibre orientation. As the possible number of experiments carried out for the present paper was limited, only specimens with fibre orientation parallel to load direction were used. However, it is very likely that the maximum number of load cycles endured by a fibre-reinforced thermoplast is depending on its fibre orientation. These effects will be taken into account within future test series.

REFERENCES

- Advani, S.G. and Tucker (1987), "The use of tensors to describe and predict fiber orientation in short fiber composites", *Journal of Rheology (1978-present)*, Vol. 31 No. 8, pp. 751–784.
- Anderson, R., Doecke, S. and Searson, D. (2009), "Vehicle age-related crashworthiness of the South Australian passenger fleet", *Centre for Automotive Safety Research*.
- Becker, F. (2009), *Entwicklung einer Beschreibungsmethodik für das mechanische Verhalten unverstärkter Thermoplaste bei hohen Deformationsgeschwindigkeiten*, Dissertation, Halle-Wittenberg, 2009.
- Blows, S., Ivers, R.Q., Woodward, M., Connor, J., Ameratunga, S. and Norton, R. (2003), "Vehicle year and the risk of car crash injury", *Injury Prevention*, Vol. 9 No. 4, pp. 353–356.
- Gruber, G., Klein, D. and Wartzack, S. (2011), "A modified approach for simulating complex compound structures within early design steps", *8th European LS-DYNA Users Conference*.
- Jollivet, T., Peyrac, C. and Lefebvre, F. (2013), "Damage of Composite Materials", *Procedia Engineering*, Vol. 66, pp. 746–758.
- Kamber, B. (2005), "Crashtest gebrauchter Fahrzeuge mit Airbag", *Dynamic Test Center Reports*.
- Kim, J.-K., Baillie, C. and Mai, Y.-W. (1992), "Interfacial debonding and fibre pull-out stresses", *Journal of Materials Science*, Vol. 27 No. 12, pp. 3143–3154.
- LANXESS Germany (2004), "Ford Focus van features hybrid metal/composite front-end", *Reinforced Plastics*, Vol. 45 No. 8, p. 4.
- Lawrence, P. (1972), "Some theoretical considerations of fibre pull-out from an elastic matrix", *Journal of Materials Science*, Vol. 7 No. 1, pp. 1–6.
- Martin, R. (2008), *Ageing of composites*, Elsevier.
- Miner, M.A. (1945), "Cumulative damage in fatigue", *Journal of applied mechanics*, Vol. 12 No. 3, pp. 159–164.
- Miner, M.A. (1959), "Estimation of fatigue life with particular emphasis on cumulative damage", *Metal Fatigue*, pp. 278–289.
- Palmgren, A. (1924), "Die Lebensdauer von Kugellagern", *Zeitschrift des Vereins Deutscher Ingenieure*, Vol. 68 No. 14, pp. 339–341.
- Short, P. and Tullo, A. (2007), "Bracing for 'K'", *Chemical & engineering news*, Vol. 85 No. 28, p. 26.
- Witzgall, C. and Wartzack, S. (2016), "Eine Untersuchung mechanisch gealterter kurzfaserverstärkter Thermoplaste unter hochdynamischen Lasten", in *DFX 2016: Proceedings of the 27th Symposium Design for X, 5-6 October 2016, Jesteburg, Germany*.
- Wu, F. and Yao, W. (2010), "A fatigue damage model of composite materials", *Fourth International Conference on Fatigue of Composites (ICFC4)*, Vol. 32 No. 1, pp. 134–138.

ACKNOWLEDGEMENTS

The authors thank the company Zwick/Roell in Ulm/Germany, particularly Johannes Künstler, for the support regarding the experiments presented in this research paper.